

Sensitivity analysis of a Small-Scale Darrieus vertical axis wind turbine

Pedro Henrique M. Barros¹, Leandro O. Salviano²

¹*Dept. of Mechanical Engineering, São Paulo State University
Ilha Solteira, 15385-000, SP, Brazil
p.barros@unesp.br*

²*Dept. of Mechanical Engineering, São Paulo State University
Ilha Solteira, 15385-000, SP, Brazil
leandro.salviano@unesp.br*

Abstract. Demand for alternative and renewable energy sources has grown substantially in recent years as a result, inter alia, of economic and environmental aspects of conventional sources such as oil and its derivatives. In this context, wind energy has emerged as attractive renewable source. The growth of wind energy in Brazil and in the world envision the possibility of developing new technologies and more efficient equipment that meet energy needs. Thus, the objective of this work is to contribute to the development of Small-Scale Darrieus Vertical Axis Wind Turbine (VAWT) that can be employed in decentralized electrical generation through computational fluid dynamics (CFD), operating at low tip speed ratio λ (TSR). A 2D numerical modeling is performed considering an unsteady-state and turbulent flow. Mesh density analysis is ensured by Grid Convergence Index (GCI) methodology and the numerical robustness is verified through experimental comparison. The geometric parameters of the VAWT analyzed are: profile camber (m), camber position (p), aerodynamic profile thickness (t), profile chord (c) and blade incidence angle (α), the first three being based on the NACA-4 digit parameterization. These five parameters, associated with the operational parameters, are submitted to a sensitivity analysis using the Smoothing Spline ANOVA algorithm in order to predict the influence of each one of these on the power coefficient (C_p) of Darrieus VAWT. With a Design of Experiments (DoE) containing 100 possible configurations of the Darrieus turbine generated using the Uniform Latin Hypercube Sampling (ULHS) method, it was possible to evaluate which parameters and interactions of them have the most influence on the power coefficient. The main finds showed that the contribution index of the angle of incidence (α) on the power coefficient was the highest among the others, with a contribution of 73%. Another significant contribution is the combination of angle of incidence parameter (α) and the profile chord (c), presenting an index of 16%. Therefore, the impact of NACA-4 digit parameterization on the power coefficient is small. Moreover, the sum of the contribution of the parameters inherent to the parameterization is only 4%.

Keywords: Wind Energy, Darrieus VAWT, Numerical Simulation, Sensitivity Analysis, NACA- 4 digit.

1 Introduction

Factors such as global warming, energy shortages, the rapid depletion of fossil fuels and the exponential growth in energy demand in several developing countries have created an excellent opportunity for the large-scale acceptance of renewable energy technology [1]. Thus, meeting the world's future energy needs results in increased pressure on conventional energy sources and their misfortunes. With rapid population growth, global energy consumption is expected to increase by 56% between 2010 and 2040. In 2015, fossil fuels (coal, oil and natural gas) accounted for 78.4% of global final energy consumption, the share being renewable energy and nuclear energy of 19.3% and 2.3%, respectively. Worldwide, the share of renewable energy will increase to face global climate change by 2030 [2]. In this scenario, the kinetic energy resulting from drafts (wind) has been an important source of energy due to its capacity for renewal and sustainability. The growth of wind energy production in Brazil and

in the world [3] envisages possibilities in the study for the development of new technologies and more efficient equipment, both in terms of large scale and in terms of small scale.

Brazil has one of the best wind resources in the world [4], exceeding the country's electricity needs by about three times. In 2017, Brazil's wind power generation reached 10% and 11% of national electricity demand in August and September, respectively [4]. Especially in the Northeast, wind energy supplied more than 60% of electricity demand, surpassing all previous generation records during a period when hydroelectric energy reservoirs in the region were very low.

In this way, the growing search for alternatives that meet the growing demand for electricity, especially for decentralized generation, and that can minimize the negative effects associated with conventional energy sources, highlight wind energy and reinforce the need for adherent research. the development of small vertical wind turbines of the Darrieus type, which appear as an attractive alternative for the generation of electricity in urban areas or isolated rural regions.

The development of this technology also contributes to the decentralized hybrid generation, associated with photovoltaic solar energy, complementing the generation in times of solar intermittence, giving the generation system robustness and reliability. In addition, the application of computational simulation tools, such as Computational Fluid Dynamics (CFD), has proven to be an excellent option for analysis and decision making, playing a fundamental role in the development of new technologies that can increase the efficiency of national projects, making them more competitive in the international market. Thus, an attractive alternative is the installation of decentralized grid systems, that is, using small-scale wind turbines, since they can generate up to 10 KW [3], which is sufficient for most domestic needs [5]. The installation of these turbines can minimize the impacts generated by the large wind farms.

The proposal for this work considers VAWTs of the Darrieus type used for decentralized energy generation in homes, small properties (especially if they are located far from the electricity distribution network), public offices, buildings or in a different urban environment. A 2D numerical modeling is performed considering an unsteady-state and turbulent flow. Mesh sensitivity analysis is ensured by Grid Convergence Index (GCI) methodology and the numerical robustness is verified through experimental comparison. The geometric parameters of the VAWT analyzed are: profile camber (m), camber position (p), aerodynamic profile thickness (t), profile chord (c) and blade incidence angle (α), the first three being based on the NACA-4 digit parameterization. These five parameters, associated with the operational parameters, are submitted to a sensitivity analysis using the Smoothing Spline ANOVA algorithm in order to predict the influence of each one of these on the power coefficient (C_p) of Darrieus VAWT.

2 Methodology

A 3-bladed VAWT with NACA-4 digit airfoils, diameter (D) equal to 1.03 mm is simulated in 2D at constant λ of 2.63. The 2D simulation represents the midplane of a turbine with high aspect ratio where the 3D tip effects are small [6]. The speed ratio λ is a ratio between the tip blade speed ωR and the freestream wind velocity U_∞ and is defined as:

$$\lambda = \omega R / U_\infty. \quad (1)$$

Darrieus wind turbine performance is a function of freestream wind velocity, U_∞ , the mechanical output power, P, the torque on the turbine axis, T, and the projected rotor area, A. By combining these parameters, we can write:

$$C_t = \frac{T}{\frac{1}{2}\rho A R U_\infty^3} \quad (2)$$

$$C_p = \frac{P}{\frac{1}{2}\rho A U_\infty^3} \quad (3)$$

where C_t and C_p are the torque coefficient and power coefficient, respectively.

A relationship between the coefficients can be written as:

$$C_p = \lambda C_t. \quad (4)$$

In this research, five geometric parameters are considered for the sensitivity analysis, namely: profile camber, m , camber position, p , aerodynamic profile thickness, t , profile chord, c , and blade incidence angle, α (see Fig. 1), the first three being based on the NACA-4 digit parameterization (see Fig. 2).

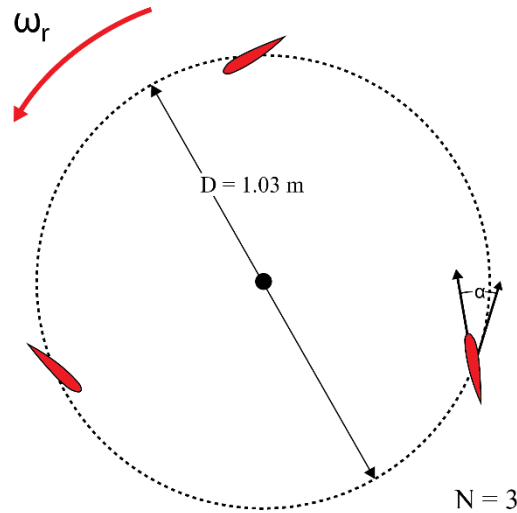


Figure 1. Representation of the geometric parameters of the turbine, namely, the diameter, D , the number of blades, N , and the angle of incidence of the blade, α

These five parameters, associated with the operational parameters, are submitted to a sensitivity analysis using the Smoothing Spline ANOVA algorithm in order to predict the influence of each one of these on the power coefficient (C_p) of Darrieus VAWT.

2.1 NACA-4 digit parameterization

For the geometric parameters of the profile, NACA-4 digit parameterization is performed, which makes a systematic representation of airfoils based on the thickness, t , profile camber, m , and its respective position, p , as shown in Fig. 2.

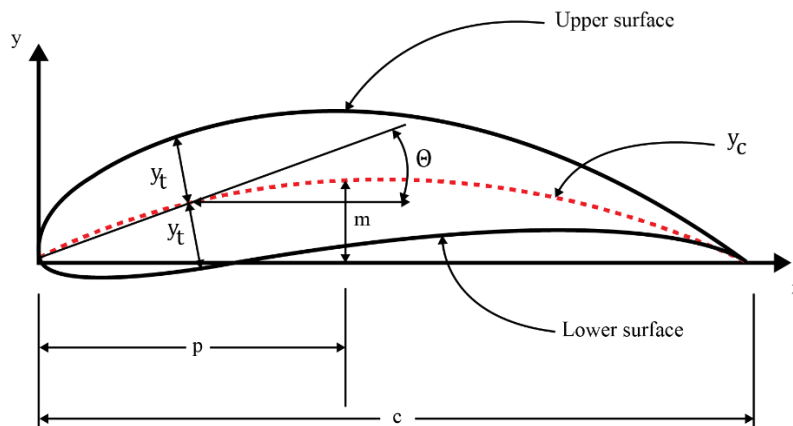


Figure 2. NACA 4-digit airfoil

The arching line y_c shown in Fig. 2 is generated from two parabola arcs, tangent to the maximum arching point m , as shown:

$$y_c = \frac{m}{(p/10)^2} \left[2x \left(\frac{p}{10} \right) - x^2 \right], x \leq (p/10), \quad (5)$$

$$y_c = \frac{m}{[1-(p/10)]^2} \left\{ \left[1 - 2 \left(\frac{p}{10} \right) \right] + 2x \left(\frac{p}{10} \right) - x^2 \right\}, x > (p/10), \quad (6)$$

where x, y_c is the pair of cartesian coordinates for each point in the arching line.

Then a modified polynomial defines the thickness distribution, y_t :

$$y_t = t(a_0\sqrt{x} - a_1x - a_2x^2 + a_3x^3 - a_4x^4), \quad (7)$$

where $a_0 = 1.4845, a_1 = 0.6300, a_2 = 1.7685, a_3 = 1.4215$ and $a_4 = 0.5075$.

The construction of the coordinates of upper surface (x_u, y_u) and of lower surface (x_l, y_l) is done by superimposing the ordinates of the thickness distribution perpendicular to the arching line, according to the following equations:

$$x_u = x - y_t(\sin \Theta), \quad (8)$$

$$y_u = y_c + y_t(\cos \Theta), \quad (9)$$

$$x_l = x + y_t(\sin \Theta), \quad (10)$$

$$y_l = y_c - y_t(\cos \Theta), \quad (11)$$

where Θ is the slope of the arching line in relation to the horizontal direction (see Fig. 2).

With the NACA-4 digit parameterization it is possible to generate symmetrical and asymmetric profiles.

2.2 Two-dimensional flow modeling

For modeling the dynamics of the two-dimensional flow of the fluid through the turbine, the Navier-Stokes equations are solved, using the Coupled algorithm [6] for the pressure-velocity coupling. Discretization is performed through the Finite Volume Methodology, considering the hypotheses of two-dimensional, incompressible, unsteady and turbulent flow. These hypotheses are suitable for modeling the flow dynamics [7]. In this way, the continuity equation can be presented in tensorial form, as shown:

$$\frac{\partial u_i}{\partial t} + \frac{\partial u_i}{\partial x_i}. \quad (12)$$

The momentum equations can be written as:

$$\frac{\partial u_i}{\partial t} + u_i \frac{\partial u_i}{\partial x_j} = -\frac{1}{\rho} \frac{\partial p}{\partial x_i} - \frac{\partial}{\partial x_j} \left[\nu \left(\frac{\partial u_i}{\partial x_j} + \frac{\partial u_j}{\partial x_i} - \frac{2}{3} \delta_{ij} \frac{\partial u_i}{\partial x_i} \right) \right] + \frac{\partial}{\partial x_j} (-\overline{u'_i u'_j}). \quad (13)$$

The turbulence model used is the Transition SST, which is based on the coupling of the transport equations $k-\omega$ SST and with two other transport equations, one for the intermittency and the other for the initial transition criterion, in terms of the number of Reynolds (Re) [8].

2.3 Computational domain and boundary conditions

In this work the Design Modeler software is used, which is a computational tool of the ANSYS Academic Research CFD package for the development of the project geometry. For this work, the fixed geometric characteristics of the wind turbine are shown in Tab. 1.

Table 1. Fixed geometric characteristics of the turbine

Characteristics	Nomenclature	Value
Turbine rotor diameter	D	1.03 [m]
Rotor height	H	1 [m] (2D simulation)
Number of blades	N	3

As the objective of the present work was to reproduce the operation of a rotating machine, it was necessary to subdivide the computational domain into three subdomains.

Thus, the computational domain consists of a rotating core, in which the turbine is located, a stationary domain involving this rotating core [6] and another circular domain that involves the blades in order to control the quality of the mesh (mainly the creation of prisms) around the aerodynamic profile. A sliding interface between the stationary domain and the rotating core allows the rotation of the turbine as shown in Fig. 3.

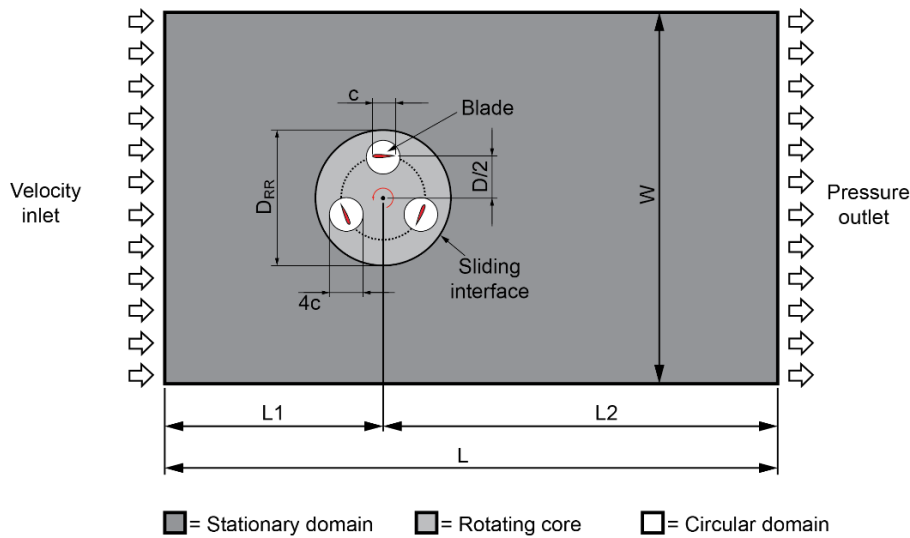


Figure 3. Computational domain with boundary conditions

The dimensions of the computational domain follow the recommendations found in the literature [6,9,10] and are represented in Tab. 2.

Table 2. Computational domain dimensions

Parameter	Nomenclature	Value
Inlet distance	L1	10D
Outlet distance	L2	15D
Rotating core diameter	D_{RR}	1,5D
Stationary domain width	W	20D

2.4 Courant number and y^+ criterion

A more in-depth understanding of the physical phenomenon can be achieved by examining the two main variables that describe the quality of numerical modeling of the flow, that is, the dimensionless distance from the wall (y^+) and the Courant Number (Co). It is common to see in the literature that a value of $y^+ \sim 1$ is adequate to describe the flow in the walls well, on the other hand, it has not been very common to find analyzes on the Courant number, which is fundamental for transient cases.

The Courant number is defined as:

$$Co = \frac{u\Delta t}{\Delta x}, \quad (14)$$

where u is the velocity of the local flow in the grid element, Δt (time-step) and Δx (dimension of a grid cell) are the temporal and spatial discretization, respectively.

When numerical simulations are performed with medium and high rotation rates, the vorticity is difficult to solve due to the strong coupling existing in the moment equations, after all, large rotation rates involve large

pressure gradients in the radial direction and this introduces difficulties in obtaining the converged solution [11]. These difficulties are further intensified by another source of inaccuracy resulting from transient numerical models; the time step must be chosen correctly to obtain reliable results. This problem leads to the widely known CFL (Courant-Friedrichs-Lewy) criterion for numerical stability, which imposes a limit on the maximum allowed value of Co and is mathematically expressed in one dimension as [11]:

$$CFL = Co < 1. \quad (15)$$

The common boundary between the rotating core and the stationary domain is defined as a conservative interface, where boundary conditions are provided. Figure 4 shows an example of this interface, composed of an unstructured triangular mesh.

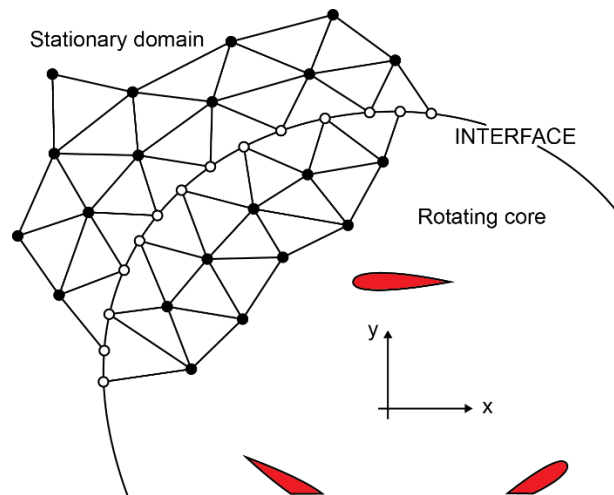


Figure 4. Interface between stationary domain and rotating core.

It is a good practice to reproduce the mesh in such a way that the elements at the interface of the fixed domain with the rotating domain have the same dimension, in this way the analysis of the Courant number is more accurate and consequently avoids numerical discrepancies [11]. We try to reproduce the mesh as shown in Fig. 4 in such a way that the elements in the interface have the same length.

Although it is theoretically valid that $Co < 1$ if the problem is studied with a linear stability analysis, when the time-step is increased, the effects of non-linearity will become prominent and oscillatory solutions may occur [12]. However, recent studies indicate that, in practice, as a general rule, the number of CFL should be as small as what is practically allowed, possibly less than 0.5 [11].

2.5 Grid convergence analysis and numerical settings

The sliding mesh model is used to capture the dynamic flow parameters due to the rotation of the turbine blades. With this, a mesh with unstructured triangular cells is created using ANSYS Meshing, as shown in Fig. 4.

The cell sizes between the fixed and rotating domains are similar to minimize numerical errors at the interface, as shown in Fig. 5. In addition, the size of the first element in the profile (Fig. 6) is defined in such a way as to meet the condition of $y^+ < 1$, which is necessary to meet the suggested criteria for the turbulence model. To better characterize the gradients over the aerodynamic profile, layers of prisms are developed, as indicated in Fig. 5. Thus, a grid with approximately 612000 elements was obtained.

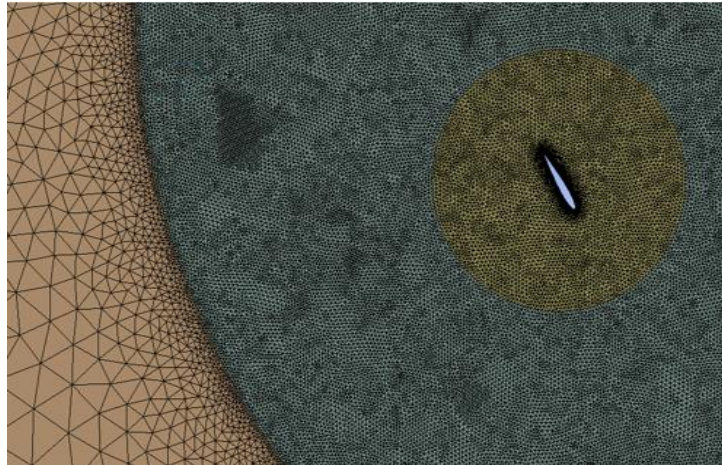


Figure 5. Computational grid at the interface between the stationary domain and rotating core.

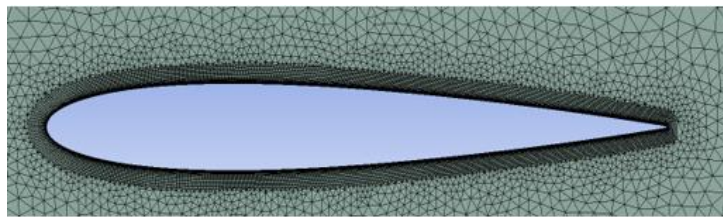


Figure 6. Layers of prismatic elements on the NACA-4 digit profile.

In order to evaluate the independence of the results due to the refinement of the computational mesh, a reference case was analyzed for three types of mesh: coarse, medium and refined. In this way, it was possible to use the Grid Convergence Index (GCI) methodology [13] to quantify the discretization errors and decide which mesh will be used in the simulations. The GCI methodology is based on the Richardson extrapolation method [14] and is widely used in CFD analysis.

The reference case used for both the GCI and the validation with experimental data is described in Tab. 3. This reference case is based on the work developed by Castelli [15].

Table 3. Main features of the validation model.

Characteristics	Nomenclature	Value
Aerodynamic profile	NACA 0021	
Profile chord	c	0.0858 [m]
Turbine rotor diameter	D	1.03 [m]
Number of blades	N	3
Inlet velocity	U_{∞}	9 [m/s]
Outlet pressure	P	1 [atm]

For this work, a GCI analysis was conducted for simulations with 0.5° angular time-step. Table 4 shows the result of the analysis. Therefore, according to Tab. 4, the numerical uncertainty in the solution between the two most refined meshes (median and refined) using the turbulence model is 0.27%. This small percentage of uncertainty justifies the choice of using the median mesh for the simulations.

Table 4. Details of the grids used for sensitivity analysis and discretization error.

Characteristics	Nomenclature	Value
Fine grid at rotating core	N_1	450.947 elements
Medium grid at rotating core	N_2	262.123 elements
Coarse grid at rotating core	N_3	152.118 elements
Power coefficient for fine grid	C_{p1}	0.303 [-]
Power coefficient for medium grid	C_{p2}	0.294 [-]
Power coefficient for coarse grid	C_{p3}	0.184 [-]
Grid Convergence Index	$GCI_{refined}^{21}$	0.268%

2.6 Smoothing Spline-ANOVA (SS-ANOVA) methodology

Smoothing spline ANOVA (SSANOVA) is a promising approach for extracting information from numerous and noisy data [16]. SSANOVAs can model multivariate data and provide nice interpretability of the modeling and prediction outcome [17]. Furthermore, assuming that the smoothing parameters are selected via cross-validation, SSANOVA models have been shown to have desirable asymptotic properties [17, 18, 19].

3 Numerical validation

To analyze the validity of the proposed numerical modeling, simulations were performed using the Transition SST turbulence model. The numerical results were compared with experimental data [15] widely disseminated in the academic community. For a first comparison, simulations were performed with an angular time-step of 1° , which is the same developed by Castelli [15], Hashem [20] and Mohamed [21]. The results are shown in Fig. 7.

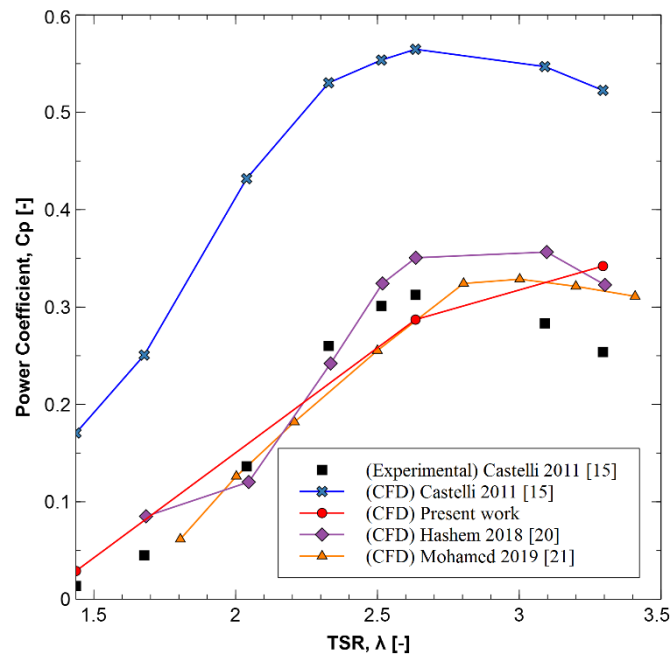


Figure 7. Numerical validation for the Darrieus turbine.

It is possible to verify that when meeting the criteria of y^+ , Co and still making a satisfactory GCI analysis, the results of the numerical simulation become sufficiently accurate for $\lambda = 2.63$.

In order to demonstrate the robustness of the numerical solution using the Transition SST turbulence model, Figure 8 shows the fulfillment of the y^+ criterion (in the turbine blades), while Fig. 9 shows the attendance of the Co (in the sliding interface) for the last revolution.

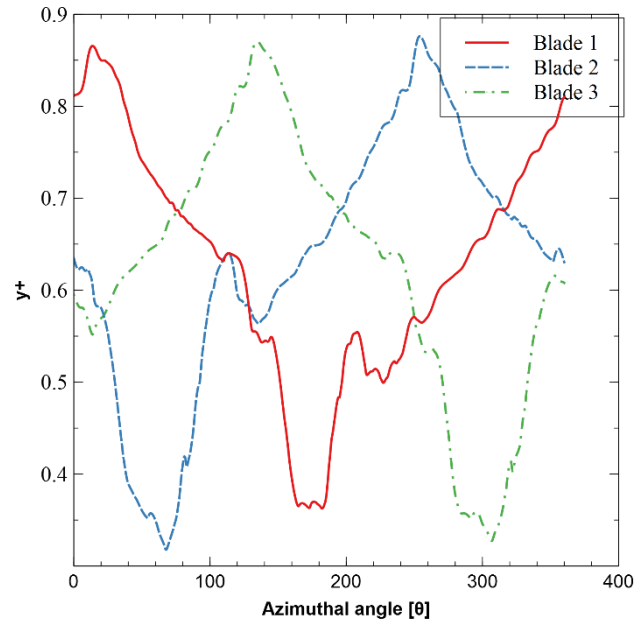


Figure 8. Fulfillment of the y^+ criterion on the blades.

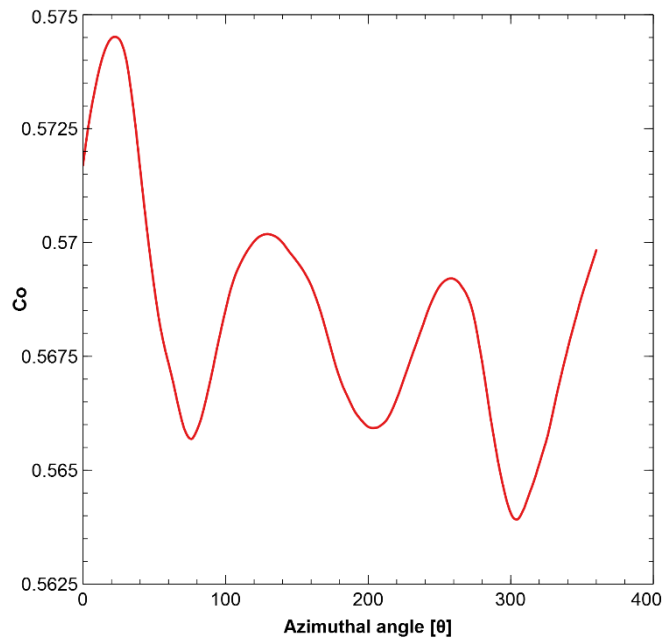


Figure 9. Co number for the last revolution.

Given the above, it is possible to observe that for the last revolution $y^+ < 1$ and on the sliding interface $Co < 1$, very close to 0.5, as recommended.

3.1 Convergence by number of revolutions

To assess the convergence, simulations were run for the same model as the validation and $TSR = 2.63$. Figure 10 shows the convergence by number of revolutions for the Transition SST model.

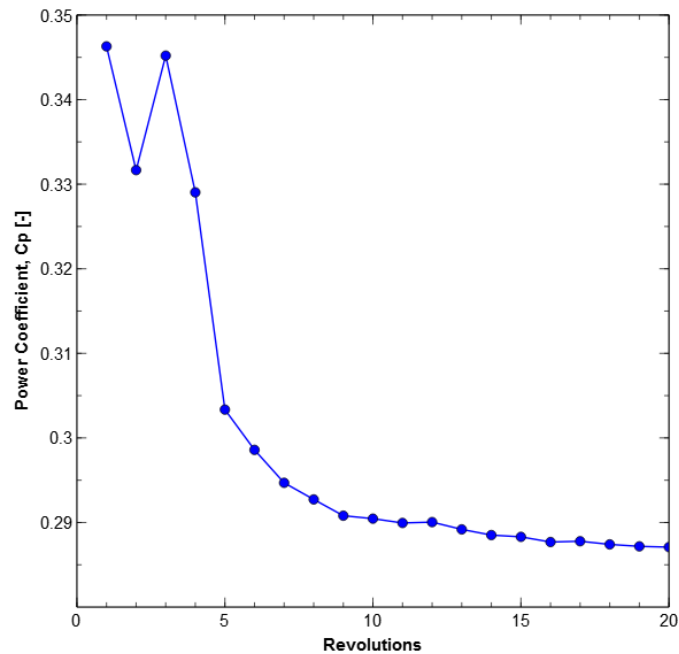


Figure 10. Convergence of the power coefficient C_p as a function of the number of revolutions.

3.2 Design of Experiments (DoE)

Design of Experiments is defined as a branch of applied statistics that deals with the planning, conduction, analysis and interpretation of controlled tests to assess the factors that control the value of a parameter or group of parameters [22]. DoE is a powerful data collection and analysis tool that can be used in various experimental situations [23]. Essentially, the DoE provides a distribution of the input variables in a sample field, thus allowing the application of statistical tools to identify the main effects and the interaction between the variables [24].

There are several approaches to determine the set of design points (unique combinations of independent variable settings) to be used in DoE. In this work, the DoE is surveyed using the Uniform Latin Hypercube Sampling (ULHS) method through ModeFrontier software.

In this work, a DoE containing 100 possible configurations of the Darrieus turbine is made considering the parameters to be analyzed and their respective operational ranges shown in Tab. 5.

Table 5. Parameters for making the DOE.

Parameters	Operational range	Increment
Profile camber (m) [-]	0 - 9	1
Camber position (p) [-]	1 - 9	1
Profile thickness (t) [-]	5 - 40	1
Profile chord (c) [mm]	50 - 200	0.5
Blade incidence angle (α) [°]	-15 - 15	0.1

4 Results

All of 100 Darrieus VAWT configurations generated using the Uniform Latin Hypercube Sampling (ULHS) method were simulated using the same boundary conditions in order to evaluate which parameters and interactions of them have the most influence on the power coefficient. Some of the results of the configurations generated by the DoE, simulated for $\lambda = 2.63$ and their respective instantaneous C_p and \bar{C}_p are shown in Fig. 11.

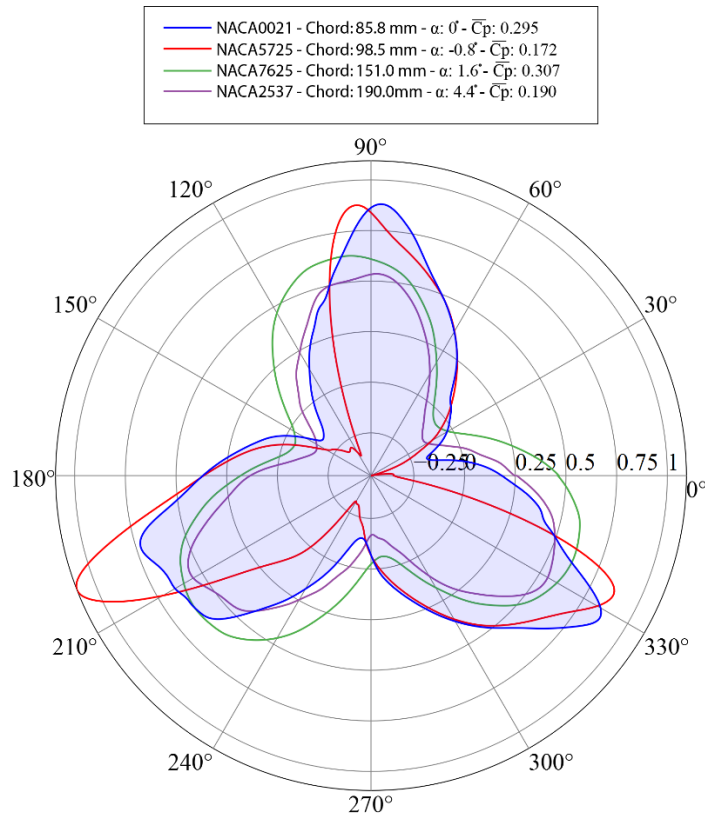


Figure 11. Comparison of instantaneous C_p and $\overline{C_p}$ for some configurations of Darrieus turbine

With this DoE containing 100 Darrieus VAWT configurations and the results of the simulation of each one it was possible to submit them to a sensitivity analysis using the Smoothing Spline ANOVA algorithm through ModeFrontier software in order to predict the influence of the parameters (input variables) described in Tab. 5 on the power coefficient (C_p). Figure 12 shows the ranking of input variables interaction effects on C_p .

The main finds showed that the contribution index of the angle of incidence (α) on the power coefficient was the highest among the others, with a contribution of 73%. Another significant contribution is the combination of angle of incidence parameter (α) and the profile chord (c), presenting an index of 16%. Therefore, the impact of NACA-4 digit parameterization on the power coefficient is small. Moreover, the sum of the contribution of the parameters inherent to the parameterization is only 4%.

In order to demonstrate the effect of the incidence angle on C_p and consecutively on $\overline{C_p}$, Fig. 13 shows the result of simulations for the same NACA profile with the same chord (c) and different incidence angle values (α). This choice was due to the fact one of these configurations presented the highest C_p on DoE and the others were just tests varying the incidence angle values in order to show the influence of this parameter on C_p .

It can be seen in Fig. 13 that the increase in the angle of incidence to a certain point tends to increase $\overline{C_p}$, but after a certain point it can mean a decrease in $\overline{C_p}$.

For a broader view of the impact of the incidence angle on the C_p , the Figures 14-17 show the velocity fields for the first two configurations in their respective points of maximum and minimum C_p reported in Fig. 13.

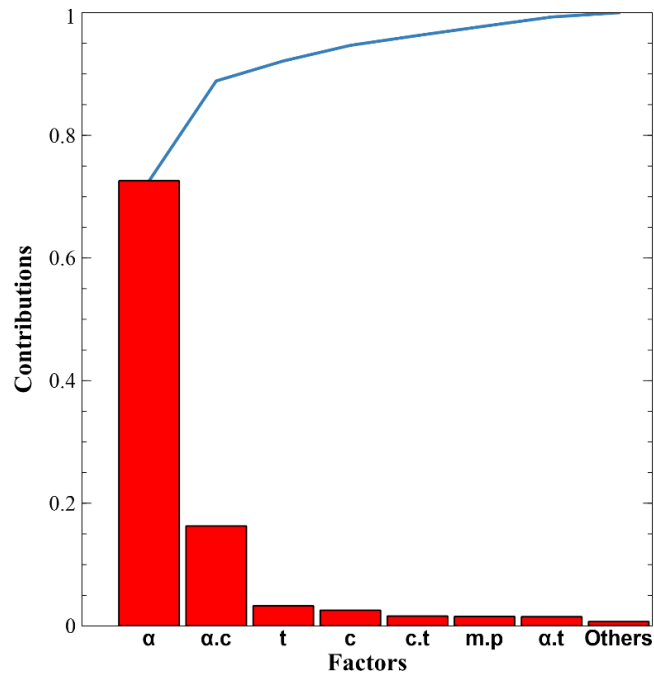


Figure 12. Ranking of input variables interaction effects

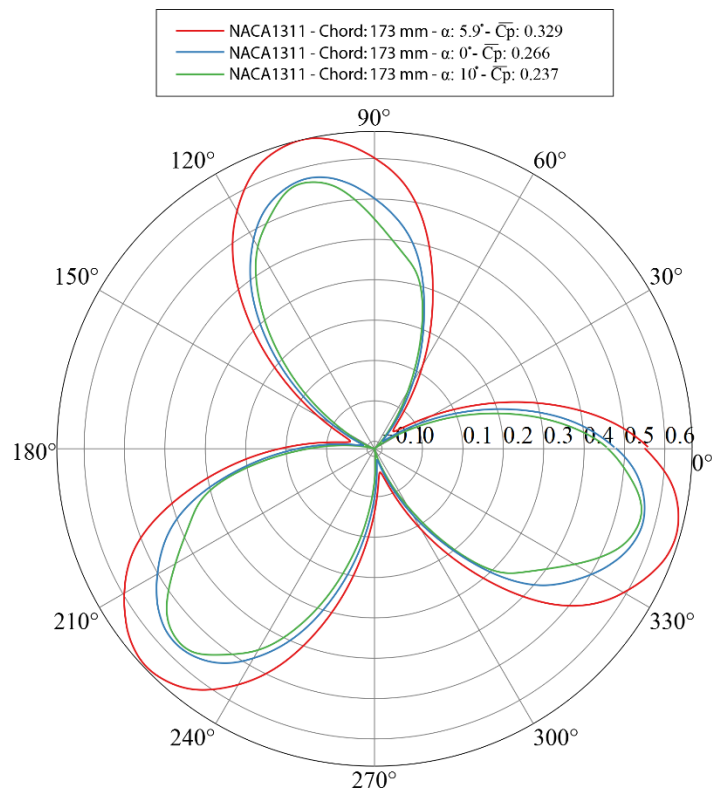


Figure 13. C_p and $\overline{C_p}$ for NACA1311 with $c = 173\text{mm}$ and different angle of incidence, α .

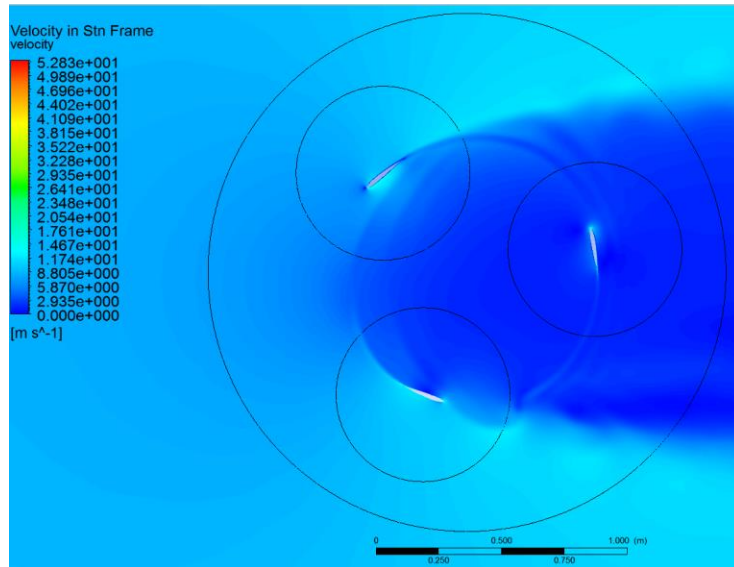


Figure 14. Velocity field for NACA1311 with $c = 173\text{mm}$ and $\alpha = 5.9$ at minimum C_p , $\theta = 45^\circ$.

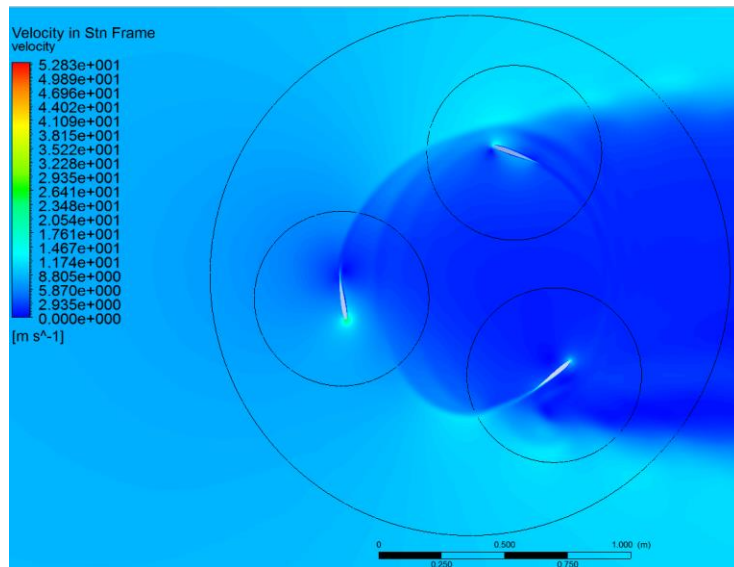


Figure 15. Velocity field for NACA1311 with $c = 173\text{mm}$ and $\alpha = 5.9$ at maximum C_p , $\theta = 105^\circ$.

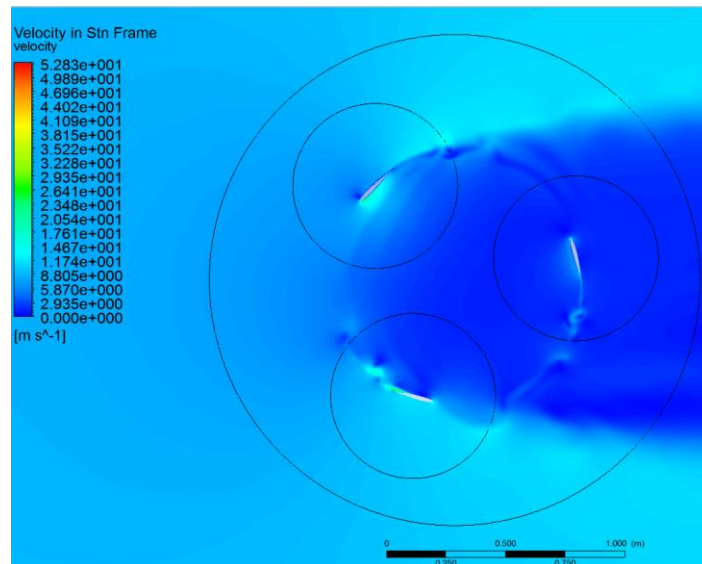


Figure 16. Velocity field for NACA1311 with $c = 173\text{mm}$ and $\alpha = 0$ at minimum C_p , $\theta = 45^\circ$.

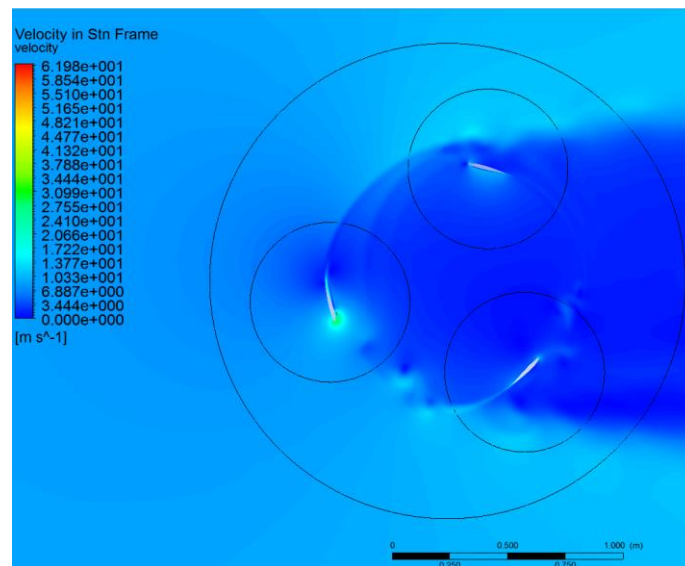


Figure 17. Velocity field for NACA1311 with $c = 173\text{mm}$ and $\alpha = 0$ at maximum C_p , $\theta = 105^\circ$.

Comparing the speed fields expressed in the previous figures, it is possible to observe that for $\alpha = 0$ there are drag zones more evident in the flow than for $\alpha = 5.9$. For this reason, there is a decrease in C_p and $\overline{C_p}$ for the configuration with $\alpha = 0$.

For the presented profile, which is asymmetrical, increasing the angle of incidence to a certain value reduces the possibility of separating the flow, causing an increase in lift force and, consequently, an increase in aerodynamic efficiency.

When the angle of incidence is zero or very high, the flow separates, causing a more disturbed wake at the trailing edge of the aerodynamic profile, decreasing the lift on the profile and increasing the drag force. This wake has an impact on the performance of the other blades during rotation, since the flow that reaches the leading edge of the other blades is disturbed.

For each profile comprised by NACA 4-digit parameterization, the angle of incidence that allows for greater and lesser aerodynamic efficiency is different, since this parameterization allows the creation of different symmetrical and asymmetric profiles. In all cases, the angle of incidence directly influences the flow around each

profile and also the flow during the rotation of the turbine causing an interaction effect between the blades.

Considering all the interactions between the studied parameters it is also possible to observe that a future optimization study can be complex, after all, there are influences due to the combinations of parameters, which makes it difficult to search for response surfaces that accurately represent the model.

Given the above, it is possible to notice that the wide operational range considered for the angle of incidence parameter compared to the small operational range of the geometric parameters of the profile contributed to its greater impact on C_p as presented in the sensitivity analysis.

5 Conclusions

A sensitivity analysis using the Smoothing Spline ANOVA algorithm in order to predict the influence of geometric input parameters of Darrieus VAWT on the power coefficient (C_p) is presented. The analysis was conducted in two-dimensional numerical simulations using ANSYS CFD considering an unsteady-state and turbulent flow. Mesh sensitivity analysis is ensured by Grid Convergence Index (GCI) methodology and the numerical robustness is verified through experimental comparison. A DoE for the geometric input parameters was done with ModeFrontier software using the Uniform Latin Hypercube Sampling and then was possible to execute the sensitivity analysis.

The work found that the contribution index of the angle of incidence (α) on the power coefficient was the highest among the others, with a contribution of 73% and another significant contribution is the combination of angle of incidence parameter (α) and the profile chord (c), presenting an index of 16%. This greater influence of the angle of incidence in C_p than the other geometric parameters is possibly related to the wide operational range considered for this parameter.

Although the influence of the geometric parameters from the NACA 4 digit parameterization in C_p is small (4%), it is not possible to say that they are irrelevant, after all, many aspects of the physical phenomenon are associated with the geometry of the aerodynamic profile.

This study shows that is possible to evaluate the changes in fluid flow behavior through the geometric parameters of a Darrieus VAWT and look for a better configuration of it.

The results of this work are valid for $TSR = 2.63$, extrapolations to other TSR values should be investigated, since no analyzes were made for such cases.

Authorship statement. The authors hereby confirm that they are the sole liable persons responsible for the authorship of this work, and that all material that has been herein included as part of the present paper is either the property (and authorship) of the authors, or has the permission of the owners to be included here.

References

- [1] R. Kumar, K. Raahemifar and A. S. Fung, "A critical review of vertical axis wind turbines for urban applications". *Renewable and Sustainable Energy Reviews*, vol. 89, pp. 281–291, 2018.
- [2] A. KC, J. Whale and T. Urmee, "Urban wind conditions and small wind turbines in the build environment: A review". *Renewable Energy*, vol. 131, pp. 268–283, 2019.
- [3] A. Tummala et al, "A review on small scale wind turbines". *Renewable and Sustainable Energy Reviews*, vol. 56, pp. 1351–1371, 2016.
- [4] S. Sawyer and M. Dyrholm, "Global Wind Energy Report: Annual Market Update 2017". Available in: <www.gwec.net>, 2018.
- [5] T. V. Hoeff et al, "A venturi-shaped roof for wind-induced natural ventilation of buildings: Wind tunnel and CFD evaluation of different design configuration". *Building and Environment*, vol. 46, pp. 1797–1807, 2011.
- [6] A. Rezaeiha, I. Kalkman and B. Blocken, "CFD simulation of a vertical axis wind turbine operating at a moderate tip speed ratio: Guidelines for minimum domain size and azimuthal increment". *Renewable Energy*, vol. 107, pp. 373–385, 2017.
- [7] C. Bai et al, "Computational fluid dynamics analysis of the vertical axis wind turbine blade with tubercle leading edge". *Journal of Renewable and Sustainable Energy*, vol. 7, n. 3, pp. 33–124, 2015.
- [8] ANSYS, "ANSYS Theory Guide". 2018.
- [9] A. Rezaeiha, H. Montazeri and B. Blocken, "Characterization of aerodynamic performance of vertical axis wind turbines: Impact of operational parameters". *Energy Conversion and Management*, vol. 169, pp. 45–77, 2018.

- [10] A. Rezaeiha, H. Montazeri and B. Blocken, “Towards accurate CFD simulations of vertical axis wind turbines at different tip speed ratios and solidities: Guidelines for azimuthal increment, domain size and convergence”. *Energy Conversion and Management*, pp. 301–316, 2018.
- [11] F. Trivellato and M. R. Castelli, “On the Courant-Friedrichs-Lewy criterion of rotating grids in 2D vertical-axis wind turbine analysis”. *Renewable Energy*, vol. 62, pp. 53–62, 2014.
- [12] F. Balduzzi et al, “Critical issues in the CFD simulation of Darrieus wind turbines”. *Renewable Energy*, vol. 85, pp. 419–435, 2016.
- [13] M. E. Meral and D. Çelik, “A flexible control strategy with overcurrent limitation in distributed generation systems”. *Electrical Power and Energy Systems*, vol. 104, pp. 456–471, 2019.
- [14] L. F. Richardson and J. A. Gaunt, “The deferred approach to the limit”. *Philos. Trans. R. Soc. London*, n. 226, pp. 299–361, 1927.
- [15] M. R. Castelli, A. Englaro and E. Benini, “The Darrieus wind turbine: Proposal for a new performance model prediction model based on CFD”. *Energy*, vol. 36, pp. 4919–4934, 2011.
- [16] N. E. Helwig and P. Ma, “Smoothing spline ANOVA for super-large samples: Scalable computation via rounding parameters”. *Statistics and its interface*, vol. 9, 2016.
- [17] C. Gu. *Smoothing Spline ANOVA Models (Second ed.)*. New York: Springer-Verlag, 2013.
- [18] K. Li, “Asymptotic Optimality for C_p , C_L , Cross-Validation and Generalized Cross-Validation: Discrete Index Set”. *The Annals of Statistics*, vol. 15, pp. 958–975, 1987.
- [19] G. Wahba. *Spline models for observational data*. Philadelphia: Society for Industrial and Applied Mathematics, 1990.
- [20] I. Hashem and M. H. Mohamed, “Aerodynamic performance enhancements of H-rotor Darrieus wind turbine”. *Energy*, vol. 142, pp. 531–545, 2018.
- [21] M. H. Mohamed, “Criticism study of J-shaped darrieus wind turbine: Performance evaluation and noise generation assessment”. *Energy*, vol. 177, pp. 367–385, 2019.
- [22] Q. Wang et al, “Statistical Design of Experiment (DoE) based development and optimization of DB213 in situ thermosensitive gel for intranasal delivery”. *International Journal of Pharmaceutics*, vol. 539, pp. 50–57, 2018.
- [23] A. S. Yang et al, “DOE-FEM based design improvement to minimize thermal errors of a high speed spindle system”. *Thermal Science and Engineering Progress*, vol. 8, pp. 525–536, 2018.
- [24] M. Nazemian, E. Neshat and R. K. Saray, “Effects of piston geometry and injection strategy on the capacity improvement of waste heat recovery from RCCI engines utilizing DoE method”. *Applied Thermal Engineering*, vol. 152, pp. 52–66, 2019.